New experimental investigation of the structure of ^{10}Be and ^{16}C by means of intermediate-energy sequential breakup

D. Dell'Aquila,[1,*] I. Lombardo,[1,†] L. Acosta,[2,3] R. Andolina,[4] L. Auditore,[5] G. Cardella,[2] M. B. Chatterjiee,[6] E. De Filippo,[2] L. Francalanza,[1] B. Gnoffo,[2] G. Lanzalone,[7,8] A. Pagano,[2] E. V. Pagano,[4,7] M. Papa,[2] S. Pirrone,[2] G. Politi,[2,4] F. Porto,[4,7] L. Quattrocchi,[5] F. Rizzo,[4,7] E. Rosato,[1,‡] P. Russotto,[2] A. Trifirò,[5] M. Trimarchi,[5] G. Verde,[2,9] and M. Vigilante[1]

[1]*Dipartimento di Fisica, Università di Napoli Federico II, and INFN-Sezione di Napoli, I-80126 Napoli, Italy*
[2]*INFN - Sezione di Catania, Via S. Sofia, I-95125 Catania, Italy*
[3]*Instituto de Física, Universidad Nacional Autónoma de México, A.P. 20-364, Mexico D.F. 01000, Mexico.*
[4]*Dipartimento di Fisica e Astronomia, Università di Catania, Via S. Sofia, I-95125 Catania, Italy*
[5]*Dipartimento di Fisica, Università di Messina and INFN - Gr. Coll. Messina, I-98166 Messina, Italy*
[6]*Saha Institute of Nuclear Physics, 700064 Kolkata, India*
[7]*INFN - Laboratori Nazionali del Sud, Via S. Sofia, I-95125 Catania, Italy*
[8]*Facolta` di Ingegneria ed Architettura, Università Kore, I-94100 Enna, Italy*
[9]*Institut de Physique Nucléaire, CNRS/IN2P3, Université Paris-Sud 11, F-91406 Orsay CEDEX, France*

^{10}Be and ^{16}C spectroscopy has been investigated by analyzing their breakup events on CH_2 and CD_2 targets. Breakup fragments have been detected by means of the CHIMERA detector. In particular, we investigated cluster decays of ^{10}Be in ^{4}He + ^{6}He and of ^{16}C in ^{6}He + ^{10}Be and ^{4}He + ^{6}He + ^{6}He. From the relative energy analysis of breakup fragments, we investigate the spectroscopy of excited states of projectile nuclei. In the ^{10}Be case we observe known states at 9.51, 10.16, 10.6, and 11.8 MeV. Further, we suggest the existence of a new state at 13.5 MeV, possibly 6^+ as indicated from angular correlation analysis. The relative energy ($E_{\rm rel} + E_{\rm th}$) spectrum of ^{16}C, reconstructed starting from ^{6}He + ^{10}Be correlations, shows a peak at about 20.6 MeV, probably related to the existence of an high-lying excited state. Non-vanishing yields are also seen in the triple coincidences ^{4}He + ^{6}He + ^{6}He.

I. INTRODUCTION

The study of cluster structure in light nuclei represents a very powerful tool for exploring the behavior of nuclear forces in few-body interacting systems [1]. For example, residual interaction between nucleons can lead to the presence of α clustering, which mostly manifests itself in the structure of light self-conjugated nuclei (^{8}Be, ^{12}C, ^{16}O, ^{20}Ne) [2]. Because of the cluster rearrangement inside nuclei, these states are usually characterized by very large deformations and peculiar shapes [3]. An example is the famous Hoyle state in ^{12}C (0^+, 7.654 MeV), for which recent experimental investigations indicate a triangular shape due to weakly bound α-like particles [4–6]. Strong deformations could characterize highly excited states in ^{16}O, where rod-like structures are predicted by various theoretical calculations [7–9].

However, cluster effects play a very peculiar role also in neutron-rich beryllium and carbon isotopes [3]. As pointed out in several papers, the extra neutrons can act to provide sort of covalent bonds between the α-like centers, contributing to an increase in the stability of the whole structure [10]. Classical examples are ^{9}Be and ^{10}Be cases that are bound, while the self-conjugated nucleus ^{8}Be is unbound. The ^{9}Be ground state is characterized by large deformation, as has been deduced from electron scattering measurements [11]. The appearance of rotational bands built on states with large moments of inertia supports the existence of molecular structure in this nucleus. For the ^{10}Be case, the situation is much more complicated and not yet fully understood [12]. 0^+ and 2^+ members of the ground-state rotational band are known, while the identification of the 4^+ state, predicted at excitation energy of about 11–12 MeV, is still uncertain [12–14]. The existence of a negative parity rotational band, with the 5.96 MeV (1^-) state as the bandhead, is known [1]. Near the energy threshold of ^{4}He + ^{6}He decay, the existence of a 0^+ state is reported. This state can be well described in terms of molecular $\alpha : 2n : \alpha$ structure. A rotational excitation of this superdeformed molecular structure is indicated by the existence of a 2^+ state at 7.54 MeV. The subsequent 4^+ member of this molecular rotational band is predicted to be located at about 10.5 MeV excitation energy. The presence of an excited state at about 10.2 MeV has been observed in the ^{7}Li(^{7}Li, ^{4}He + ^{6}He) ^{4}He reaction [15]. Curtis *et al.* assigned $J^\pi = 3^-$ to this state via angular correlation measurements [16]. This assignment was subsequently contradicted in Ref. [17] and in recent ^{6}He + ^{4}He inverse kinematic resonant elastic scattering experiments [18,19], where a 4^+ assignment is made. This state could therefore be the 4^+ member of the molecular rotational band. Very recently, preliminary results obtained in a new resonant elastic scattering experiment at the Array for Nuclear Astrophysics and Structure with Exotic Nuclei (ANASEN) facility at Florida State University [19] tentatively suggest the existence of a 6^+ excited state in ^{10}Be at about 13.6 MeV. This

*dellaquila@na.infn.it
†ivlombardo@na.infn.it
‡Deceased.

state could represent a new member of the cluster band in ^{10}Be [20]. Molecular bands have been clearly observed also for the ^{11}Be [1] and ^{12}Be [21–23] neutron-rich isotopes, pointing out the common nature of clusterization effects in isotopic chains of light nuclei.

Cluster effects of molecular nature are predicted also in excited states of neutron-rich carbon isotopes. Interesting studies have been done recently on ^{13}C [24–26] and ^{14}C [27] structures via resonant elastic scattering in direct and inverse kinematics. In this context, ^{16}C has recently attracted a large interest because of its possible linear molecular structure [28,29]. The presence of a 4 valence neutron, possibly correlated into two $2n$ couples by pairing effects, could increase the stability of linear or triangular three-center α-cluster structure. Theoretical calculations performed with the antisymmetrized molecular dynamics (AMD) model supported this hypothesis, pointing out also the parity-asymmetric nature of a possible linear chain structure (e.g., a ^{10}Be $+\alpha+2n$ like configuration) [30]. Unfortunately, very few experimental data have been reported on the spectroscopy of ^{16}C at excitation energy values around the cluster disintegration thresholds at 16.5 MeV (^{6}He $+$ ^{10}Be) and 22.9 MeV (^{8}He $+$ ^{8}Be) [31,32]. For this reason, no definitive conclusions can be drawn because of the lack of experimental data.

In the present paper we report new results on the spectroscopy of ^{10}Be and ^{16}C excited states above the cluster emission thresholds. In both cases, breakup reactions of radioactive projectiles have been used to explore the structure of these nuclei. Breakup fragments have been detected by the CHIMERA array. A relative energy analysis of correlated fragments allows us to inspect the structure of ^{10}Be and ^{16}C nuclei, pointing out the possible presence of unreported excited states. In particular, we found indications of a possible state at about 13.5 MeV in ^{10}Be, as it is seen from the ^{4}He $+$ ^{6}He coincidence data. The angular correlation analysis points out a high spin value (possibly 6^+) for this state, confirming the findings of [19]. For the ^{16}C nucleus, the ^{6}He $+$ ^{10}Be coincidence data suggest the presence of a new state at about 20.6 MeV, possibly predicted in [30], even if the statistics are too low to perform angular correlation analysis. Nonvanishing yield is also seen for the ^{6}He $+$ ^{6}He $+$ ^{4}He triple coincidence data.

II. EXPERIMENTAL DETAILS

The experiment was performed at the In Flight Radioactive Ions Beams (FRIBs) facility of INFN-Laboratori Nazionali del Sud (LNS) (Catania, Italy). The fragmentation beam was produced starting from a 55 MeV/nucleon ^{18}O primary beam accelerated by the LNS K-800 Superconducting Cyclotron. A 1.5 mm thick ^{9}Be target was used for fragments production. They are subsequently selected in magnetic rigidity ($B\rho\approx$2.8 T m) via the LNS Fragment Separator, with a momentum acceptance of $\Delta p/p \approx 0.01$. In this way, a cocktail beam with high intensity of ^{16}C at 49.5 MeV/u ($\approx 10^5$ particles per second), ^{13}B ($\approx 5\times10^4$ pps), and ^{10}Be at 56 MeV/u ($\approx 4\times10^4$ pps) can be delivered on various targets for physics experiments. A tagging system [33], made by a microchannel plate (MCP) detector and a double-sided silicon strip detector

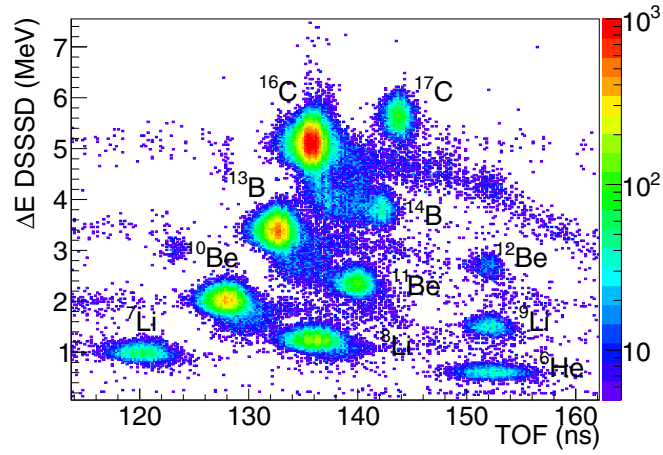

FIG. 1. Identification plot of the FRIBs cocktail beam. Each radioactive ion beam (indicated by label) is located in a well-defined region in (TOF, ΔE DSSSD) plane. The finite resolution is due to the combination of detector resolution and LNS Fragment Separator momentum acceptance.

(DSSSD, 140 μm thick), installed along the beam line, was used to identify each incoming isotope produced by projectile fragmentation. An identification of fragmentation products is obtained by correlating the energy loss in the DSSSD and the time of flight (TOF) needed to cover the flight path from the MCP to the DSSSD detector ($\approx$13 m). As shown in Fig. 1, this tagging system allows a good isotopic separation of beam particles. The position of the cocktail beam on the target was determined by using a tracking system based on two position sensitive DSSSD. The beam spot size on the target was of the order of 1.5 $\times$ 1.5 cm^2 with an angular spread of 1°.

To induce projectile breakup reactions we used a 50 μm polyethylene $(CH_2)_n$ target. In some runs a 28 μm deuterated polyethylene $(CD_2)_n$ target was also used. The breakup products from the ^{1}H(^{10}Be, ^{4}He ^{6}He), ^{2}H(^{10}Be , ^{4}He ^{6}He), ^{12}C(^{10}Be , ^{4}He ^{6}He), and ^{1}H(^{16}C , ^{6}He ^{10}Be), ^{2}H(^{16}C , ^{6}He ^{10}Be), ^{12}C(^{16}C, ^{6}He ^{10}Be) reactions were detected by using the 4π multidetector CHIMERA [34,35]. It comprises 1192 Si-CsI(Tl) telescopes, covering $\simeq$94% of the whole solid angle. The first stage of the telescope has a 300 μm thick silicon detector and it is followed by a CsI(Tl) crystal, having a thickness from 6 to 12 cm in length, depending on the angular position in the detector, and readout by a photodiode. Further details about the array and its detection and identification capabilities are described in Refs. [35–37]. In the present experiment we used the first three forward rings of the CHIMERA array, covering the polar angle range $2.2^\circ \leqslant \theta \leqslant 6.4^\circ$, with a sufficiently good granularity for this experiment (varying from 0.133 to 0.458 msr at increasing polar angle). As reported in [38], the projectile breakup cross section is forward peaked; therefore we expect to detect a large amount of fragments coming from projectile breakup in the present angular domain. Detailed efficiency calculations, performed with Monte Carlo techniques, will be shown in the following sections for the two cases of ^{10}Be and ^{16}C breakup processes.

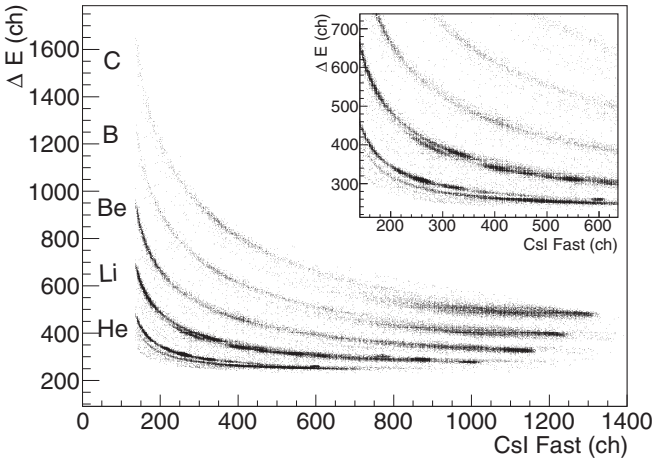

FIG. 2. ΔE-E spectrum obtained at $\theta_{\rm lab} = 3.1^\circ$. The x-axis values are proportional to the residual energy released in the second E detection stage [CsI(Tl) scintillator], while the y-axis values represent the energy loss in the Si first stage ΔE detector (in channels). The insert shows a magnified view of the same identification plot.

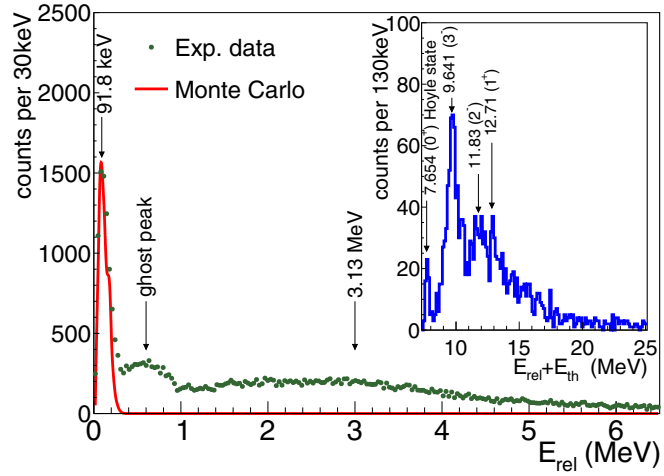

FIG. 3. ^{8}Be relative energy spectrum from the α-α correlations (green points). The red line is the result of a Monte Carlo simulation considering ^{8}Be disintegration from the ground state. Insert shows the ^{12}C relative energy ($E_{\rm rel} + E_{\rm th}$) spectrum obtained from the 3α correlations. Arrows indicate the energy position of ^{12}C known states reported in literature. The low-energy narrow peak is compatible with the Hoyle state.

Si and CsI(Tl) detectors of the CHIMERA array were calibrated via elastic scattering of various light ion beams impinging on a polyethylene target. Great care has been taken in the CsI(Tl) calibration. The dependence of the CsI(Tl) response on the mass and charge of incident particles [39] was taken into account by using the parametrization given in [40], as discussed in detail in Ref. [41]. Charge and mass identification of fragments was based on the ΔE-E technique. A typical particle identification matrix is shown in Fig. 2. The lines corresponding to different nuclear species, from helium to carbon, are clearly identified. As seen in the insert of Fig. 2, ^{4}He and ^{6}He can be unambiguously identified. Reasonable isotopic identifications can be also obtained up to beryllium isotopes. In particular, in the case of beryllium, the main contribution to the scatter plot comes from the ^{10}Be line, ending with the ^{10}Be elastic scattering peak.

III. EXPERIMENTAL RESULTS

To reconstruct the excitation energy of the decaying nuclear states, we analyzed kinematical correlations between couples of breakup fragments coming from the inelastic excitation of ^{10}Be and ^{16}C projectiles. In particular, by measuring their masses, energies, and emission angles, we reconstructed the kinetic energy of the two breakup fragments in the reference frame of the emitting nucleus. The corresponding excitation energy was obtained by adding the rest mass of the exit breakup channel with respect to the emitting nucleus ground state (energy threshold, $E_{\rm th}$) to the measured total kinetic energy in the emitting nucleus frame (relative energy, $E_{\rm rel}$). Details about this technique can be found, for example, in Refs. [16,42–44].

As a preliminary check of our experimental technique we analyzed the case of α-α and 3α correlations. In the first case, the obtained relative energy spectrum, reported in Fig. 3, shows a narrow peak at about 0.09 MeV, clearly compatible with the emission from the ^{8}Be ground state. This evidence is supported by the result of a Monte Carlo simulation (red line), obtained with the assumptions described in the following section. A wide bump also appears centered at about 3 MeV, an indication of the 3.04 MeV 2^+ state of ^{8}Be. The *ghost peak* (≈0.6 MeV), caused by the decay by neutron emission of the ^{9}Be 2.43 MeV $5/2^-$ state, is also present in analogy to [45], confirming the consistency of the procedure. Interesting results have been obtained also from the triple coincidences. In this case we can investigate the disintegration of ^{12}C via 3α emission. The corresponding relative energy spectrum is shown in the insert of Fig. 3. Arrows indicate the position of known states in ^{12}C. In particular, the narrow peak at low energies, well separated from the large peak at 9.64 MeV due to the 3_1^- state, is evidence of the 3α disintegration of ^{12}C from the Hoyle state.

A. ^{10}Be case

When a projectile nucleus impinges on a CH_2 target, one can induce reactions on C or H nuclei, with important changes in the reaction kinematics and in the dominant involved reaction mechanism. If we consider the coincidences of ^{4}He and ^{6}He fragments in our data, an inspection of the Q-value spectrum obtained by momentum conservation and assuming a carbon recoil shows the appearance of a narrow peak centered around the Q_{ggg} value (i.e., −7.409 MeV), that corresponds to breakup reactions induced by inelastic scattering on carbon, and a broader low-lying peak, in analogy to [38]. This peak is shifted to the Q_{ggg} value if we assume a recoiling hydrogen. As discussed in [38], this behavior is useful in discriminating between the two target components.

The excitation energy of the ^{10}Be nucleus has been therefore reconstructed via the ^{4}He + ^{6}He cluster breakup channel, from the relative energy of the two fragments. Since we do not observe significant differences in the excitation energy spectra from the two target contributions (CH_2 and

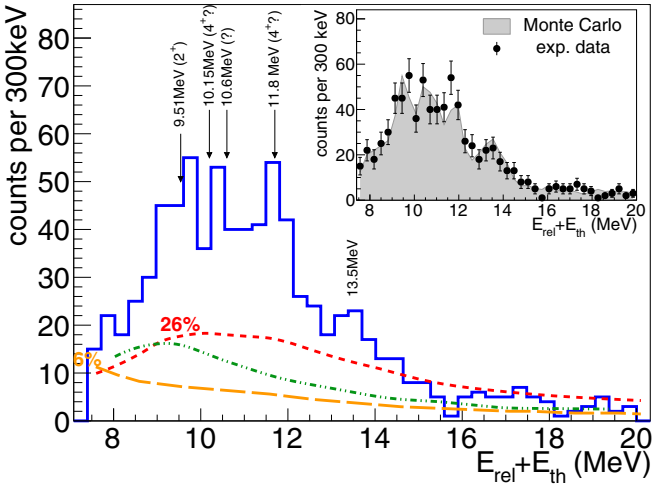

FIG. 4. ^{10}Be relative energy ($E_{\rm rel} + E_{\rm th}$) spectrum obtained from the ^{4}He + ^{6}He decay channel. Vertical arrows indicate the energies of known states of this nucleus. In round brackets we plot the J^π assignment taken from the literature. The dashed lines represent the simulated detection efficiencies obtained by assuming hydrogen recoil (red dotted line) or carbon recoil (orange dashed line). The green dashed-dotted line is the uncorrelated background estimated by an event mixing procedure. The insert shows the results of a Monte Carlo simulation obtained by considering the contributions of the excited states listed in Table I, compared to the experimental data (black points with error bars).

CD_2), in order to increase the statistics we report in Fig. 4 the relative energy ($E_{\rm rel} + E_{\rm th}$) spectrum obtained by summing the data from both targets. The vertical arrows in Fig. 4 indicate the energies of ^{10}Be excited states known in the literature (as discussed in Sec. I and reported in Table I). Despite the low statistics and limited relative energy resolution, they are in agreement with the present data. It is very interesting to observe that the appearance of a bump at $E_x \simeq 13.5$ MeV suggests the possible fingerprint of a new, unreported state in ^{10}Be. To check if the observed peak can be really ascribed to the existence of an excited state in ^{10}Be or is due to different effects, we evaluated the expected background (due to spurious coincidences) and the detection efficiency.

As a first approximation, the background can be described by considering the contribution of uncorrelated couples of particles (event mixing). The background due to event mixing, shown in Fig. 4 with the green dashed-dotted line, was calculated by selecting couples of ^{4}He and ^{6}He coming from different events of reaction induced by all the isotopes of the cocktail beam.

TABLE I. ^{10}Be level structure from ^{4}He + ^{6}He breakup channel.

E_x (MeV)	J^π	$\Gamma_{\rm tot}$ (MeV)
9.51	2^+ [38,45,53]	0.14 [16,31]
10.6[31]		0.20 [15,16]
11.8	(4^+)[31,52]	0.12 [31,52]
$\simeq$13.5	(6^+)[19], this work	($<$0.35) this work

The detection efficiency (dashed lines in different colors) was estimated by performing a Monte Carlo simulation of the CHIMERA multidetector. As suggested in the literature [38,43,46] the angular distribution of inelastic scattering at intermediate energies can be approximately described by the formula $\frac{d\sigma}{d\Omega_{\rm c.m.}} \propto \exp(-\frac{\theta_{\rm c.m.}}{\alpha})$, where α is a fall-off factor of the order of 12°–16°. Two different efficiency curves have been obtained by taking into account the interaction of projectiles with hydrogen (red dotted curve in Fig. 4) and carbon (orange dashed curve in Fig. 4). The trends of the two estimated efficiency curves are different because of the different scattering kinematics: at $E_x = 10$ MeV in ^{10}Be, the limiting angle for scattering on hydrogen is about 5.2°, while for scattering on carbon there is no limiting angle. Therefore, the geometrical coverage of the first three rings of the CHIMERA array leads to higher detection efficiency in the case of the hydrogen target because of the more forward-focused kinematics. In all cases, the shapes of the event mixing background and of the efficiency curves are very smooth and should not lead to the presence of spurious peaks in the relative energy spectrum. For these reasons we suggest attributing the 13.5 MeV bump to the decay from an excited state in ^{10}Be.

This state would be energetically compatible with the missing 6^+ member of the ^{10}Be molecular rotational band, studied in [17], and made of the 6.179 MeV state as a 0^+ member, the 7.542 MeV as a 2^+ member, and the 10.2 MeV state (observed also in this experiment) as a possible 4^+ member. Spin and parity of the suggested 13.5 MeV state can be tentatively estimated via angular correlation analysis in terms of Legendre polynomials [47–49]. Figure 5 shows the $|\cos\Psi'|$ distribution for the 13.5 MeV peak, where $\Psi' = \Psi + \Delta\Psi$, with Ψ the angle formed by the relative velocity vector of the two detected fragments with the beam axis and $\Delta\Psi$ the phase shift correction, as discussed for example in [21,48–50]. The last term can be calculated via the relation $\Delta\Psi = \frac{\ell_i - J}{J}\theta_{\rm c.m.}$, where ℓ_i is the angular momentum of the dominant partial wave in the entrance channel, J is the spin of the resonance, and $\theta_{\rm c.m.}$ is the inelastic scattering angle in the center-of-mass frame. The $\theta_{\rm c.m.}$ angle can be estimated by means of kinematics calculations; the nature of recoiling targets can be discriminated with selections on the Q-value spectrum. Considering that at intermediate energies, inelastic scattering processes have essentially a direct and peripheral nature, only a narrow window of angular momenta centered around the grazing value ℓ_g would contribute to the scattering amplitude because of the short range of the nuclear part of the interaction [50]. For this reason, we can assume $\ell_i \approx \ell_g$ as a first approximation. The ℓ_g has been calculated with the Wilcke model [51]. For example, in the present case we have $\ell_g \approx 10\hbar$ for the proton target.

The behavior of the experimental data, shown for the 11.8 MeV bump in the case of $J = 4$ assignment [Fig. 5(a)] and for the 13.5 MeV bump in the case $J = 6$ [Fig. 5(b)] assignment, is compared with the theoretical prediction $W(\theta^*, \Psi) \propto |P_J(\cos\Psi')|^2$, where P_J are the Legendre polynomials of J order; this theory is valid for spinless particles in the exit channel. Because all the known excited states of ^{6}He decay by particle emission with $t_{1/2} \geqq 5.8 \times 10^{-21}$ s (a

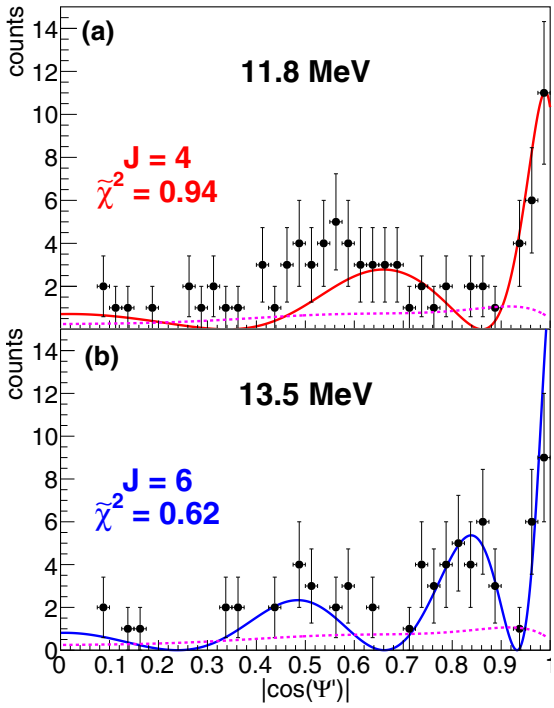

FIG. 5. Angular correlation distribution of ^{4}He + ^{6}He breakup channel for the 11.8 MeV (a) and for the 13.5 MeV (b) bumps seen in the ^{10}Be relative energy ($E_{rel} + E_{th}$) spectrum, compared with the expected angular distribution assuming (a) $J = 4$ (red line) and (b) $J = 6$ (blue line). The theoretical angular distributions are corrected for the detection efficiency, presented with the magenta dashed line. The corresponding reduced χ^2 are also indicated for each case.

factor $\approx 10^{12}$ times smaller than the typical time of flight of detected particles), the direct detection of ^{6}He breakup fragments entails that we are observing ^{6}He produced in their 0^+ ground state. The theoretical curves (solid lines) have been corrected for the calculated detection efficiency, estimated via a Monte Carlo simulation (shown by the magenta dashed lines). Moreover, the Legendre polynomials being squared even functions, i.e., $|P_J(\cos\Psi')|^2 = |P_J(|\cos\Psi'|)|^2$, we have presented the $|\cos\Psi'|$ distribution, instead of $\cos\Psi'$, in order to increase the statistics. As an example, this procedure can be applied to the 11.8 MeV state, for which the literature suggests a possible $J^\pi = 4^+$ assignment [31,52]. The corresponding angular correlation, shown in the top panel, partially agrees with the theoretical curve for a 4^+ assignment. The discrepancies can be attributed to the presence of a non-negligible background or to contributions of close-lying states with different J_π.

A similar analysis has been carried out for the 13.5 MeV state; experimental angular correlation has been compared with theoretical predictions for various J values from 0 to 8. Based on χ^2 analysis, the best fit of data is obtained assuming $J^\pi = 6^+$ ($\tilde{\chi}^2 = 0.62$). Despite the low statistics and the presence of background, the agreement is reasonably good as visible in Fig. 5(b).

As a final test of the present analysis, we performed a complete Monte Carlo simulation of the experiment considering all the states listed in Table I and assuming that, as a first approximation, the reaction mechanism leads to equal state population. We have also taken into account the J^π of each state by considering the corresponding angular correlation. The simulated spectrum has been normalized to the area of the experimental one. The result is shown in the insert of Fig. 4 by the shaded histogram, which is in nice agreement with the experimental data (black dots). These calculations point out that at ≈13.5 MeV excitation energy, the relative energy resolution of the experimental device is ≈0.45 MeV. In this way we can give an upper limit of ≈0.35 MeV for the 13.5 MeV state width.

It is interesting to observe that the possible existence of a 13.5 MeV 6^+ state in ^{10}Be has been suggested by the recent observations on resonant elastic scattering reported in Ref. [19], where the J^π of the 13.5 MeV peak is estimated by means of R-matrix fit of experimental data. On the contrary, a recent (^{18}O, ^{17}O) neutron transfer investigation [54] seems to point out no marked evidence of ^{10}Be states in this energy region. This finding could indicate the α cluster nature of the 13.5 MeV state in ^{10}Be, being that the α resonant elastic scattering and the cluster breakup techniques particularly sensitive to give evidence of α cluster states (especially of a molecular nature, thanks to the pronounced $\alpha + 2n$ structure of ^{6}He), while neutron transfer reactions are usually more focused on the selection of single-particle excitations.

B. ^{16}C case

The ^{16}C structure was investigated by analyzing the ^{10}Be + ^{6}He breakup channel. In analogy to the ^{10}Be case, the Q-value spectrum was calculated assuming both carbon and hydrogen recoils. In both cases a bump close to the corresponding Q_{ggg} value (−16.505 MeV) is seen.

As discussed for the ^{10}Be case, the excitation energy of ^{16}C before decaying can be deduced from the relative energy of the two breakup fragments (^{10}Be and ^{6}He in the case here studied). Combining the data of both targets we found the spectrum reported in Fig. 6(a). In this case, due to the very low accumulated statistics, we cannot reasonably estimate the background contribution with the event mixing procedure. The presence (even with poor statistics) of a narrow peak at about 20.6 MeV represents the possible signature of an unreported excited state in ^{16}C. The red and orange dashed curves are the simulated detection efficiencies by assuming hydrogen or carbon recoil respectively and the same functional form of the inelastic scattering angular distribution used for the ^{10}Be case. The efficiency curves exhibit quite smooth trends. Therefore the peak at $E_{rel} + E_{th} \approx 20.6$ MeV should not be attributed to effects related to the detection efficiency. Another interesting point is that also previous works [28,29] show a yield enhancement at about 21 MeV of ^{16}C excitation energy, as evident in the insert of Fig. 5. Our data are characterized by higher statistics as compared to previous experiments. Very interesting is also the fact that in this excitation energy region, theoretical calculations of Ref. [30] have predicted the possible presence of various 6^+ states, members of two triangular

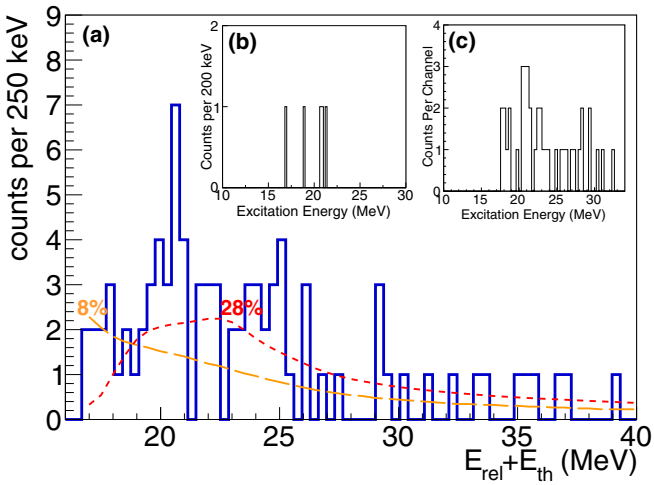

FIG. 6. (a) ^{16}C relative energy ($E_{\rm rel} + E_{\rm th}$) spectrum obtained from the ^{10}Be + ^{6}He breakup channel. Orange dashed line: Monte Carlo simulated detection efficiency obtained by assuming ^{12}C recoils. Red dotted line: Monte Carlo simulated detection efficiency obtained by assuming ^{1}H recoils. Details on the Monte Carlo calculations are discussed in the text. (b) ^{16}C excitation energy spectrum obtained from the ^{10}Be + ^{6}He breakup channel, as reported in Ref. [29]. (c) ^{16}C excitation energy spectrum obtained from the ^{10}Be + ^{6}He breakup channel, as reported in Ref. [28].

bands and of a linear chain band. Unfortunately, given the low statistics collected in our experiment, we cannot exclude its attribution to phase-space decay without assumption of any state and we are unable to investigate the angular correlation for the 20.6 MeV bump.

Finally, it is also possible to explore the structure of ^{16}C via three-body cluster breakup channels. Following the suggestions of the literature [28] we studied the ^{6}He + ^{6}He + ^{4}He breakup channel, which gives a very small number of coincidences. The Q-value spectrum for these events, obtained by assuming hydrogen recoils, shows a broad bump centered around the Q_{gggg} (−23.914 MeV) value. Including all the selected ^{6}He + ^{6}He + ^{4}He triple coincidences, without any cut on the Q-value spectrum, we found the relative energy spectrum shown with black dashed line in Fig. 7. In the same figure we show with a green filled histogram the same relative energy spectrum gated within the Q-value window $Q = Q_{gggg} \pm 30$ MeV. Despite the very low statistics, the relative energy ($E_{\rm rel} + E_{\rm th}$) spectrum shows an enhanced yield at about 34 MeV. Indeed the gate on the Q value seems to slightly reduce the yield in proximity to the 34 MeV peak and to completely cut the coincidence yield over 40 MeV. This high-energy region has been also studied in Ref. [30], indicating the possible presence of the 12^{+} member of the above discussed linear chain band.

Because of the very low statistics, this finding needs further investigations. If the existence of a high-energy state in ^{16}C, visible via three-body breakup, will be confirmed, it would be the first indication of three-body cluster disintegration of ^{16}C, since the literature [28] does not provide the evidence of this rare process.

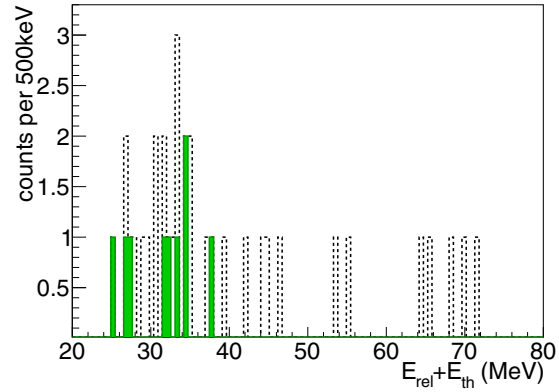

FIG. 7. ^{16}C relative energy ($E_{\rm rel} + E_{\rm th}$) spectrum for the three-body ^{6}He + ^{6}He + ^{4}He breakup channel. The black dashed histogram represents the relative energy ($E_{\rm rel} + E_{\rm th}$) spectrum obtained without cuts on the Q value. The green filled histogram is obtained by gating the reconstructed Q value (assuming hydrogen recoils) in the range $Q = Q_{gggg} \pm 30$ MeV.

IV. CONCLUSIONS

In conclusion, the structures of ^{10}Be and ^{16}C have been investigated via projectile breakup reactions using cocktail radioactive fragmentation beams. First, we investigated the ^{10}Be* → ^{6}He + ^{4}He breakup channel; from this analysis we found the presence of known excited states and also the possible indication of a new state at about 13.5 MeV. Angular correlation analysis of the 13.5 MeV peak tentatively suggests a possible 6^{+} spin-parity assignment for this state. Our finding seems in agreement with a very recent work [19], where ^{6}He + ^{4}He elastic scattering was studied. This 13.5 MeV state could be compatible in energy with the expected 6^{+} missing member of the ^{10}Be molecular rotational band investigated in [17].

The structure of ^{16}C was investigated via the ^{10}Be + ^{6}He and ^{6}He + ^{6}He + ^{4}He decay channels. In the first case we found a yield enhancement at about 20.6 MeV excitation energy that seems to be consistent with results obtained in other low statistics measurements [28,29]. This finding could be related to the excitation of a state near 21 MeV, but because of the limited statistics, we cannot exclude its attribution to phase-space decay without assumption of any state. In the second case, an enhancement of the triple coincidence yield is seen at about 34 MeV. In both cases a new measurement with better statistics is needed to confirm the present experimental findings.

We plan to carry out new experiments at the FRIBs facility with improved statistics by taking advantage of a future upgrade of the primary beam current. Further, we will improve the reconstruction of relative energy by coupling CHIMERA with a new high-granularity hodoscope, the femtoscope array for correlations and spectroscopy (FARCOS) [55], placed at forward angles. These points will allow us to obtain firmer spectroscopic information on light nuclei far from the stability line.

ACKNOWLEDGMENTS

We gratefully acknowledge Drs. D. Rifuggiato and G. Cosentino and the whole accelerator team of INFN-Laboratori Nazionali del Sud, Catania, for their help in the production and transport of the radioactive beam. We thank also C. Marchetta and E. Costa for handling and manufacturing the production and reaction targets.

[1] W. Von Oertzen, M. Freer, and Y. Kanada-En'yo, Phys. Rep. **432**, 43 (2006).

[2] K. Ikeda, N. Tagikawa, and H. Horiuchi., Prog. Theor. Phys. Suppl. **E68**, 464 (1968).

[3] C. Beck, *Clusters in Nuclei* (Springer, Heidelberg, 2013), Vols. 1–3.

[4] M. Freer and H. O. U. Fynbo, Prog. Part. Nucl. Phys. **78**, 1 (2014).

[5] D. J. Marin-Lambarri, R. Bijker, M. Freer, M. Gai, T. Kokalova, D. J. Parker, and C. Wheldon, Phys. Rev. Lett. **113**, 012502 (2014).

[6] W. R. Zimmermann, M. W. Ahmed, B. Bromberger, S. C. Stave, A. Breskin, V. Dangendorf, T. Delbar, M. Gai, S. S. Henshaw, J. M. Mueller, C. Sun, K. Tittelmeier, H. R. Weller, and Y. K. Wu, Phys. Rev. Lett. **110**, 152502 (2013).

[7] T. Suhara, Y. Funaki, B. Zhou, H. Horiuchi, and A. Tohsaki, Phys. Rev. Lett. **112**, 062501 (2014).

[8] T. Ichikawa, J. A. Maruhn, N. Itagaki, and S. Ohkubo, Phys. Rev. Lett. **107**, 112501 (2011).

[9] Y. Kanada-En'yo, Phys. Rev. C **91**, 034303 (2015).

[10] W. Von Oertzen, Z. Phys. A **357**, 355 (1997).

[11] D. Vinciguerra and T. Stovall, Nucl. Phys. A **132**, 410 (1969).

[12] H. T. Fortune and R. Sherr, Phys. Rev. C **84**, 024304 (2011).

[13] N. I. Ashwood, N. M. Clarke, M. Freer, B. R. Fulton, R. J. Woolliscroft, W. N. Catford, V. A. Ziman, R. P. Ward, C. J. Bickerton, C. E. Harrison, and V. F. E. Pucknell, Phys. Rev. C **68**, 017603 (2003).

[14] H. G. Bohlen, T. Dorsch, T. Kokalova, W. von Oertzen, C. Schulz, and C. Wheldon, Phys. Rev. C **75**, 054604 (2007).

[15] N. Soić *et al.*, Europhys. Lett. **34**, 7 (1996).

[16] N. Curtis, D. D. Caussyn, N. R. Fletcher, F. Marechal, N. Fay, and D. Robson, Phys. Rev. C **64**, 044604 (2001).

[17] M. Freer, E. Casarejos, L. Achouri, C. Angulo, N. I. Ashwood, N. Curtis, P. Demaret, C. Harlin, B. Laurent, M. Milin, N. A. Orr, D. Price, R. Raabe, N. Soić, and V. A. Ziman, Phys. Rev. Lett. **96**, 042501 (2006).

[18] D. Suzuki, A. Shore, W. Mittig, J. J. Kolata, D. Bazin, M. Ford, T. Ahn, F. D. Becchetti, S. BeceiroNovo, D. BenAli, B. Bucher, J. Browne, X. Fang, M. Febbraro, A. Fritsch, E. Galyaev, A. M. Howard, N. Keeley, W. G. Lynch, M. Ojaruega, A. L. Roberts, and X. D. Tang, Phys. Rev. C **87**, 054301 (2013).

[19] G. V. Rogachev *et al.*, J. Phys.: Conf. Ser. **569**, 012004 (2014).

[20] R. Wolski *et al.*, Phys. At. Nucl. **73**, 1405 (2010).

[21] M. Freer, J. C. Angelique, L. Axelsson, B. Benoit, U. Bergmann, W. N. Catford, S. P. G. Chappell, N. M. Clarke, N. Curtis, A. DArrigo, E. deGoesBrennard, O. Dorvaux, B. R. Fulton, G. Giardina, C. Gregori, S. Grevy, F. Hanappe, G. Kelly, M. Labiche, C. LeBrun, S. Leenhardt, M. Lewitowicz, K. Markenroth, F. M. Marques, M. Motta, J. T. Murgatroyd, T. Nilsson, A. Ninane, N. A. Orr, I. Piqueras, M. G. SaintLaurent, S. M. Singer, O. Sorlin, L. Stuttge, and D. L. Watson, Phys. Rev. Lett. **82**, 1383 (1999).

[22] R. J. Charity, S. A. Komarov, L. G. Sobotka, J. Clifford, D. Bazin, A. Gade, L. Jenny, S. M. Lukyanov, W. G. Lynch, M. Mocko, S. P. Lobatov, A. M. Rogers, A. Sanetullaev, M. B. Tsang, M. S. Wallace, S. Hudan, C. Metelko, M. A. Famiano, A. H. Wuosmaa, and M. J. van Goethem, Phys. Rev. C **76**, 064313 (2007).

[23] Z. H. Yang, Y. L. Ye, Z. H. Li, J. L. Lou, J. S. Wang, D. X. Jiang, Y. C. Ge, Q. T. Li, H. Hua, X. Q. Li, F. R. Xu, J. C. Pei, R. Qiao, H. B. You, H. Wang, Z. Y. Tian, K. A. Li, Y. L. Sun, H. N. Liu, J. Chen, J. Wu, J. Li, W. Jiang, C. Wen, B. Yang, Y. Liu, Y. Y. Yang, P. Ma, J. B. Ma, S. L. Jin, J. L. Han, and J. Lee, Phys. Rev. C **91**, 024304 (2015).

[24] M. Milin and W. von Oertzen, Eur. Phys. J. A **14**, 295 (2002).

[25] M. Freer, N. I. Ashwood, N. Curtis, A. DiPietro, P. Figuera, M. Fisichella, L. Grassi, D. JelavicMalenica, T. Kokalova, M. Koncul, T. Mijatovic, M. Milin, L. Prepolec, V. Scuderi, N. Skukan, N. Soic, S. Szilner, V. Tokic, D. Torresi, and C. Wheldon, Phys. Rev. C **84**, 034317 (2011).

[26] I. Lombardo, L. Campajola, E. Rosato, G. Spadaccini, and M. Vigilante, Nucl. Instrum. Meth. Phys. Res. B **302**, 19 (2013).

[27] M. Freer, J. D. Malcolm, N. L. Achouri, N. I. Ashwood, D. W. Bardayan, S. M. Brown, W. N. Catford, K. A. Chipps, J. Cizewski, N. Curtis, K. L. Jones, T. Munoz-Britton, S. D. Pain, N. Soic, C. Wheldon, G. L. Wilson, and V. A. Ziman, Phys. Rev. C **90**, 054324 (2014).

[28] P. J. Leask, J. Phys. G: Nucl. Part. Phys. **27**, B9 (2001).

[29] N. I. Ashwood *et al.*, Phys. Rev. C **70**, 064607 (2004).

[30] T. Baba, Y. Chiba, and M. Kimura, Phys. Rev. C **90**, 064319 (2014).

[31] Brookhaven National Laboratory, National Nuclear Data Center, http://www.nndc.bnl.gov/.

[32] H. G. Bohlen, R. Kalpakchieva, B. Gebauer, S. M. Grimes, H. Lenske, K. P. Lieb, T. N. Massey, M. Milin, W. vonOertzen, C. Schulz, T. Kokalova, S. Torilov, and S. Thummerer, Phys. Rev. C **68**, 054606 (2003).

[33] I. Lombardo *et al.*, Nucl. Phys. B (Proc. Suppl.) **215**, 272 (2011).

[34] E. De Filippo and A. Pagano, Eur. Phys. J. A **50**, 32 (2014).

[35] A. Pagano, Nucl. Phys. News **22**, 25 (2012).

[36] N. Le Neindre *et al.*, Nucl. Instrum. Methods Phys. Res. A **490**, 251 (2002).

[37] M. Alderighi *et al.*, Nucl. Instrum. Methods Phys. Res. A **489**, 257 (2002).

[38] M. Freer, J. C. Angelique, L. Axelsson, B. Benoit, U. Bergmann, W. N. Catford, S. P. G. Chappell, N. M. Clarke, N. Curtis, A. DArrigo, E. deGoesBrennard, O. Dorvaux, B. R. Fulton, G. Giardina, C. Gregori, S. Grevy, F. Hanappe, G. Kelly, M. Labiche, C. LeBrun, S. Leenhardt, M. Lewitowicz, K. Markenroth, F. M. Marques, J. T. Murgatroyd, T. Nilsson, A. Ninane, N. A. Orr, I. Piqueras, M. G. SaintLaurent, S. M. Singer, O. Sorlin, L. Stuttge, and D. L. Watson, Phys. Rev. C **63**, 034301 (2001).

[39] A. Wagner *et al.*, Nucl. Instrum. Methods Phys. Res. A **456**, 290 (2001).

[40] D. Horn *et al.*, Nucl. Instrum. Methods Phys. Res. A **320**, 273 (1992).
[41] L. Acosta *et al.*, Nucl. Instrum. Methods Phys. Res. A **715**, 56 (2013).
[42] J. van Driel, Phys. Lett. B **98**, 351 (1981).
[43] A. G. Artyukh *et al.*, Instr. Exp. Tech. **52**, 13 (2009).
[44] N. I. Ashwood, M. Freer, J. C. Angelique, V. Bouchat, W. N. Catford, N. M. Clarke, N. Curtis, O. Dorvaux, F. Hanappe, Y. Kerckx, M. Labiche, J. L. Lecouey, F. M. Marques, T. Materna, A. Ninane, G. Normand, N. A. Orr, S. Pain, N. Soic, L. Stuttge, C. Timis, A. Unshakova, and V. A. Ziman, Phys. Rev. C **70**, 024608 (2004).
[45] S. Ahmed, M. Freer, J. C. Angelique, N. I. Ashwood, V. Bouchat, W. N. Catford, N. M. Clarke, N. Curtis, F. Hanappe, J. C. Lecouey, F. M. Marques, T. Materna, A. Ninane, G. Normand, N. A. Orr, S. Pain, N. Soic, C. Timis, A. Unshakova, and V. A. Ziman, Phys. Rev. C **69**, 024303 (2004).
[46] H. G. Bohlen *et al.*, Z. Phys. A **308**, 121 (1982).
[47] M. Freer, Nucl. Instrum. Methods Phys. Res. A **383**, 463 (1996).
[48] S. Marsh and W. D. M. Rae, Phys. Lett. B **153**, 21 (1985).
[49] A. Cunsolo, A. Foti, G. Imme, G. Pappalardo, G. Raciti, and N. Saunier, Phys. Rev. C **21**, 2345 (1980).
[50] G. R. Satchler, *Direct Nuclear Reactions* (Oxford University, Oxford, 1983), p. 553.
[51] W. W. Wilcke *et al.*, At. Data Nucl. Data Tab. **25**, 389 (1980).
[52] D. R. Tilley *et al.*, Nucl. Phys. A **745**, 155 (2004).
[53] N. Curtis, N. I. Ashwood, L. T. Baby, T. D. Baldwin, T. R. Bloxham, W. N. Catford, D. D. Caussyn, M. Freer, C. W. Harlin, P. McEwan, D. L. Price, D. Spingler, and I. Wiedenhover, Phys. Rev. C **73**, 057301 (2006).
[54] D. Carbone, M. Bondi, A. Bonaccorso, C. Agodi, F. Cappuzzello, M. Cavallaro, R. J. Charity, A. Cunsolo, M. DeNapoli, and A. Foti, Phys. Rev. C **90**, 064621 (2014).
[55] G. Verde *et al.*, J. Phys. Conf. Ser. **420**, 012158 (2013).